"Probucol ameliorates renal and metabolic sequelae of primary CoQ deficiency in *Pdss2* mutant mice"

SUPPLEMENTARY MATERIAL INDEX:

Supporting Information File 1. CoQ_{10} treatment duration effects in B6.*Pdss2*$^{kd/kd}$ missense mutant mice. Although only three animals were studied following short-term treatment with CoQ_{10} from day of life 104, they had significantly more urine albumin than did the group treated from weaning that were an average of one month younger at analysis. In contrast to the effectiveness of short-term treatment with probucol initiated around day 100 (**Table II**), treatment with CoQ_{10} over the same time interval did not have a significant effect. *, p values were determined by Mann-Whitney U test relative to mice treated with CoQ_{10} from weaning.

Supporting Information File 2. ^{31}P-NMR analysis of lipid extract obtained from the liver of wild-type and *Pdss2* mutant mice fed either standard chow or supplemented long-term with either probucol or CoQ_{10}. **(A)** Liver lipid composition in B6.*alb/cre,Pdss2*$^{loxP/loxP}$ liver-conditional knockout mutants fed standard chow alone ("alb/cre") or following long-term probucol supplementation ("alb/cre + probucol") relative to healthy controls on standard chow ("LoxP"). Cardiolipin content was 80% increased in B6.*Alb/cre,Pdss2*$^{loxP/loxP}$ liver-conditional knockout mutant mice relative to LoxP healthy controls, and normalized (decreased) with probucol treatment. **(B)** Total phospholipid content and relative proportion of cardiolipin and phosphatidyl choline in liver extracts from LoxP, alb/cre, and alb/cre + probucol mice. Probucol reduced total liver extract sphingomyelin and phospholipid content in liver-conditional knockout, leading to a relatively increased percent cardiolipin of the total phospholipid pool in knockout mutants. **(C)** Liver lipid composition in B6.*Pdss2*$^{kd/kd}$ missense mutants fed standard chow alone (kd/kd) or following supplementation with either probucol ("kd/kd + probucol") or CoQ_{10} supplementation ("kd/kd + CoQ_{10}") separated by gender relative to healthy controls fed

standard chow ("B6"). Although total cardiolipin content appeared unchanged in the B6.*Pdss2*$^{kd/kd}$ missense mutants relative to B6 controls, cardiolipin was below the limit of detection by NMR analysis of pooled liver extracts from the probucol-treated missense mutant mice. While CoQ_{10} treatment had no effect on cardiolipin content in missense mutant mice, it appeared to modestly increase hepatic liver phosphatidyl ethanolamine, phosphatidyl choline, and plasmalogens . **(D)** Total phospholipid content and relative proportion of cardiolipin and phosphatidyl choline in liver extracts from B6, kd/kd, kd/kd + probucol, and kd/kd + CoQ_{10} separated by gender. Probucol reduced total liver extract sphingomyelin and phospholipid content in missense mutant mice. Y-axis indicates nMol/gram wet weight of ground liver tissue. Each bar represents combined liver extract from two replicate animals per strain and treatment. PtE, phosphatidyl ethanolamine, PtL, phosphatidyl lysine; LysoPtC, lysophosphatidyl choline; PtC, phosphatidyl choline; Plas, plasmalogen; PL, phospholipid; CL, cardiolipin.

Supporting Information File 3. Mitochondrial lipid peroxidation in isolated liver and kidney mitochondria from *Pdss2* missense mutant and liver-conditional knockout mice was unchanged from wild-type and not altered by long-term drug treatments. Anti-4-HNE Western blot analysis of 20 to 40 ug isolated mitochondrial protein demonstrated no qualitative difference in cumulative lipid peroxidation as a marker of reactive species damage in isolated liver mitochondria from **(A)** B6.*Pdss2*$^{kd/kd}$ (kd/kd) male missense mutants (aged 148 to 154 days), or **(B)** B6.*alb/cre,Pdss2*$^{loxP/loxP}$ (alb/cre) liver-conditional knockout male mice (aged 178 to 213 days) relative to respective healthy B6 or LoxP male controls. **(C)** Anti-4-HNE labeling in a separate cohort of female *Pdss2* missense mutant mice (aged 141 to 154 days) similarly showed no difference in the overall staining intensity or pattern in isolated mitochondria from either *liver* (lane 1: B6 control, lane 2: kd/kd), as above, or *kidney* (lane 5: B6 control, lane 6: kd/kd) in missense mutant mice. Nor did long-term treatment of missense mutant animals with either probucol or CoQ_{10} qualitatively alter the pattern in either *liver* (lane 3: kd/kd + probucol, lane 4: kd/kd + CoQ_{10}) or *kidney* (lane 7: kd/kd + probucol; lane 8: kd/kd + CoQ_{10}). *Lane sample description* (all females): 1, B6 liver 215 days old; 2, kd/kd liver 141 days old; 3, kd/kd liver 145 days old; 4, kd/kd liver 154 days old; 5, kd/kd kidney 215 days old; 6, kd/kd kidney 142 days old; 7, kd/kd

kidney 145 days old; 8, kd/kd kidney 154 days old. (**D**) Immunoblot staining with the mitochondrial loading control, VDAC1 (MW:30 kDa), showed equivalent loading of samples described in (C).

Supporting Information File 4. Analysis of hepatic function in liver-conditional *Pdss2* knockout mice on chronic probucol therapy. B6.*alb/cre,Pdss2*$^{loxP/loxP}$ (*"alb/cre"*) liver-conditional knockout mice exhibited no evidence of liver damage based on plasma ALT levels in animals on standard chow with or without probucol supplementation. Blood glucose was significantly elevated in *alb/cre* liver conditional knockout mutants ($p < 0.05$), and significantly decreased with probucol fed to the animals from weaning. Urea was not significantly different among the groups. Although blood ammonia was unaltered in *alb/cre* liver-conditional knockout mice relative to B6.*Pdss2*$^{loxP/loxP}$ ("LoxP") controls, probucol significantly decreased blood ammonia relative to both untreated *alb/cre* mutants and age-matched healthy controls. All measurements were obtained following 4 hour fasts. Combined data across all ages of each strain and treatment group are indicated in bold font. *, $p < 0.05$ and ***, $p < 0.001$ relative to combined LoxP control. $^{\#}$, $p < 0.05$ and $^{\%}$, $p < 0.001$ relative to *alb/cre* mutant on standard diet.

Supporting Information File 5. Excel summary of all significant <u>pathway-level</u> transcript alterations in *Pdss2* mutant mice without treatment and following long-term supplementation with either probucol CoQ_{10} relative to wild-type controls. Normalized enrichment scores (NES) and statistical analyses of all reported microarray data is provided for each pair-wise comparison analyzed for relative expression changes among KEGG-defined pathways by Gene Set Enrichment Analysis (GSEA). Data includes comparisons in both B6.*Pdss2*$^{kd/kd}$ missense mutant and B6.*alb/cre,Pdss2*$^{loxP/loxP}$ liver-conditional knockout mutants. Treatment group comparisons are made both to untreated mutants and to wild-type healthy controls. Expression microarray files used to generate these results are accessible in NCBI GEO (GSE18677 and GSE27954).

Supporting Information File 6. Complex I-dependent respiratory capacity in permeabilized skeletal muscle fibers from B6.*Pdss2*$^{kd/kd}$ missense mutant mice was not increased by long-term probucol therapy. No increase in complex I-dependent (malate+glutamate+ADP) or complex I+II dependent

(malate+glutamate+ADP+succinate) respiratory capacity was seen in permeabilized muscle from B6.*Pdss2*$^{kd/kd}$ mice following long-term probucol therapy. Age-matched B6.*Pdss2*$^{kd/kd}$ untreated vs. long-term probucol treated mice were studied in parallel on two consecutive days by high resolution respirometry (Oroboros, Austria). **(A)** Comparison of integrated respiratory capacity in permeabilized muscle fibers from an untreated, 206 day old B6.*Pdss2*$^{kd/kd}$ male vs. a 203 day old B6.*Pdss2*$^{kd/kd}$ male treated with probucol from weaning. **(B)** Comparison of integrated respiratory capacity in permeabilized muscle fibers from an untreated 203 day old B6.*Pdss2*$^{kd/kd}$ female vs. a 205 day old B6.*Pdss2*$^{kd/kd}$ male treated with probucol from weaning. Interestingly, the untreated female mutant had higher complex I-dependent respiratory capacity than was observed in the untreated male mutant.

Supporting Information File 7. Gene-level expression analysis of antioxidant pathways in *Pdss2* mutants. Genes categorized by gene ontology terms 'antioxidant activity', 'peroxidase activity', and 'glutathione peroxidase activity' were used to generate gene sets for GSEA analysis. The zip file includes all GSEA comparison results, where the "Index" file within each folder provides an overview of pathway-level results for each comparison. The excel spreadsheet within the zip file provides results of gene-level expression changes of antioxidant pathways in *Pdss2* mutant mice (both 'kd/kd' missense mutants and 'alb/cre' liver-conditional knockout mice) at baseline and following long-term treatment with either probucol or CoQ_{10} relative to healthy controls. "Untr-Ctrl", compares untreated kd/kd to B6; "Prob-Untr", compares probucol-treated kd/kd to untreated kd/kd; "CoQ-Untr", compares CoQ_{10}-treated kd/kd to untreated kd/kd; "Affy-Mut", compares untreated alb/cre knockouts to LoxP controls; "Affy-Treat", compares probucol-treated alb/cre knockouts to untreated alb/cre knockouts. In each comparison, upregulated or downregulated genes in the first group relative to the second are indicated by positive or negative expression values, respectively. Values represent mean log2-transformed expression measurements.

Supporting Information File 8. **Heme oxygenase gene-level expression analysis in *Pdss2* mutants.** *HMOX1* and *HMOX2* gene expression assessed by Illumina genome-wide expression profiling were not significantly altered in B6.*Pdss2*$^{kd/kd}$ missense mutant mice relative to B6 wild-type control animals, nor

affected by long-term treatment with either probucol or CoQ_{10}. While B6.*alb/cre,Pdss2*$^{loxP/loxP}$ liver-conditional knockout mutants analyzed by Affymetrix U133_P2 arrays had significantly increased *HMOX1* expression in liver relative to wild-type, probucol therapy did not significantly alter expression of either heme oxygenase gene. Log2-transformed expression measurements of individual mice do not reflect absolute expression levels due to platform differences. P values were generated by student's t-test.

Supporting Information File 9. Heatmap view of gene-level analysis among significantly altered biochemical pathways in *Pdss2* mutant mice relative to wild-type and following therapy with either probucol or CoQ_{10}. Heatmap comparison at the individual gene level provides a gross overview of metabolic effects from the two mutation types and individual treatments among the most significantly and concordantly altered KEGG-defined pathways. Genes are represented by individual columns, where boxes denote gene clusters comprising a single KEGG-defined metabolic pathway. Each row represents results of a given pair-wise microarray comparison, where red and green indicate relative up- or downregulation in the first group compared to the second, respectively, and color intensity conveys significance. In all heatmaps shown, row 1 indicates comparison of alb/cre knockout mice ("KO") vs loxP wild-type controls ("WT"); row 2, missense mutants ("kd/kd") vs B6 wild-type controls ("WT"); row 3, alb/cre knockout mice treated with probucol vs untreated alb/cre knockout mice; row 4, missense mutants treated with probucol vs untreated missense mutants; and row 5, missense mutants treated with CoQ_{10} relative to untreated missense animals. Raw and processed gene-level data is accessible at NCBI GEO (GSE18677 and GSE27954).

This view reinforces that liver-conditional *Pdss2* knockouts significantly upregulate expression of a host of intermediary metabolic pathways (8), as well as *PPAR* pathway signaling. While missense mutants upregulated OXPHOS pathway genes, significantly decreased expression was seen for many other basic metabolic pathways including *PPAR* signaling and fatty acid metabolism. Probucol therapy in missense mice significant upregulated both of these pathways, whereas CoQ_{10} therapy significantly upregulated only fatty acid metabolism. Reversal of expression alterations following probucol therapy was even more dramatic on pathways involved in protein processing and catabolism of multiple amino acids. Indeed, protein processing

involving ribosome, protein export, and proteasome pathways were significantly upregulated in both mutant typess, while amino acid catabolism pathways were significantly upregulated in knockouts and downregulated in missense mutants. All of these changes were significantly reversed toward expression levels seen in wild-type by both drugs, but to a greater extent by probucol. Other pathways with significantly altered expression in *Pdss2* mutants fell into the categories of immune pathways and cell defense. In alb/cre knockouts, probucol significantly downregulated toward wild-type levels expression of pathways involved in steroid biosynthesis, P450 metabolism, and bisphenol A degradation pathways. By contrast, missense mutants had upregulated immune pathways but mainly downregulated cell defense pathways, all of which was largely normalized by either probucol or CoQ_{10}. Nucleotide metabolism, which was largely upregulated in both mutant types, was significantly downregulated in the direction of wild-type by either CoQ_{10} or probucol treatment.

Supporting Information File 10. Integrated gestalt of global metabolic alterations that occur in primary mitochondrial dysfunction is depicted in KEGG Atlas images of the mouse B6.*Pdss2*$^{kd/kd}$ missense mutant (**Panel A**) and B6.*alb/cre,Pdss2*$^{loxP/loxP}$ liver-conditional knockout ("alb/cre KO") mutant (**Panel B**), where each illustrates pathway-level expression results relative to wild-type. While several pathways were similarly upregulated in both mutant types, the vast majority of metabolic pathways showed significantly discordant expression. Probucol therapy dramatically reversed the direction of altered expression particularly in missense mutants (**Panel C**) but also in liver-conditional knockout mutants (**Panel D**), almost globally across all areas of intermediary metabolism, illustrated by clear reversal of color within many individual pathways. Lines represent enzymes, nodes represent metabolic substrates, relative up-or down-regulation is denoted by red and green coloring, respectively, and line color intensity conveys significance. Visually demonstrating the interconnectedness of observed effects on intermediary metabolism, circled groupings indicate a. OXPHOS, b. tricarboxylic acid cycle, c. pyruvate metabolism, d. glycolysis, e. carbohydrate metabolism, f. fatty acid metabolism, g. steroid biosynthesis, h. nucleotide metabolism, i. amino acid metabolism, j. urea cycle, and k. cellular defense pathways.

Supporting Information File 11. Heatmap of gene-level expression alterations within the *PPAR* signaling

pathway in *Pdss2* mutant mice. Rows represent individual pathway genes, with gene names listed to the right of the heatmap. Columns represent drug and treatment groups. Dotted blue line separates mutation effects in untreated B6.*Alb/cre,Pdss2*$^{loxP/loxP}$ ("*alb/cre*") liver conditional knockout mutants and B6.*Pdss2*$^{kd/kd}$ ("*kd/kd*") missense mutants relative to wild-type control animals, respectively, from treatment effects of probucol ("prob") in *alb/cre* and of either probucol or CoQ_{10} ("CoQ") in *kd/kd*. All treatments were provided from weaning. Red and green indicate up-or downregulated in the first group relative to the second, respectively. Color intensity conveys significance. Black or purple arrows respectively highlight the three *PPAR* family transcription factors (α, δ, and γ) and their key downstream target genes in fat metabolism (*CPT2*, *LPL*).

Supporting Information File 12. Gender effect of long-term probucol supplementation on CoQ_9 and CoQ_{10} content in liver. A gender effect was evident when comparing CoQ_9 and CoQ_{10} liver levels. CoQ_9 and CoQ_{10} content was measured in liver extracts of B6.*Pdss2*$^{kd/kd}$ missense mutant mice at baseline and following long-term probucol supplementation from birth. Female missense mutants had an approximately 2-fold higher liver content of both CoQ_9 ($p < 0.01$) and CoQ_{10} ($p < 0.001$) than did males at baseline. Long-term probucol supplementation significantly increased liver CoQ_{10} content in both females ($p < 0.01$) and males ($p < 0.0001$), with 46% greater absolute levels achieved on average in females (2.95 +/- 0.8 pmol/mg protein in probucol-treated females and 2.02 +/- 0.80 pmol/mg protein in probucol-treated males). Similar effects were seen for CoQ_9 levels, which were 40% greater on average in probucol-treated females (76.6 +/- 19.24 pmol/mg protein) than males (54.68 +/- 17.81 pmol/mg protein). However, increased liver CoQ_9 content in probucol-treated missense mice only reached a significant level of change relative to untreated missense mutants in males ($p < 0.0001$). Gender, age at sacrifice, CoQ content, urine albumin (mg protein/24 hours), and nephritis score are indicated for each animal. P value was determined for CoQ_9 and CoQ_{10} content by student's t-test between gender-matched probucol-treated and untreated animals.

Supporting Information File 1. CoQ_{10} treatment duration effects in B6.*Pdss2*$^{kd/kd}$ missense mutant mice.

Treatment Group	N (f,m)	Age at Sacrifice	Nephritis Score	Nephritis p value*	Urine Albumin (mg/24 hour)	Albumin p value*
CoQ_{10} from Weaning	10 (4, 6)	124 +/- 4.03	1.7 +/- 0.64		3.37 +/- 1.91	
CoQ_{10} from Day 98	4 (0, 4)	117 +/- 0	0.67 +/- 0.47	0.06	3.07 +_/- 1.31	0.48**
CoQ_{10} from Day 104	3 (2,1)	151 +/- 0.94	2.33 +/- 0.47	0.21	12.09 +/- 1.72	0.007

* p value determined by Mann-Whitney U test relative to mice treated with CoQ_{10} from weaning.

** These 4 males excreted 5.01 +/- 1.71 mg albumin at day 98, and then were given CoQ_{10} for 19 days. At day 117, they excreted 3.07 +/- 1.31 mg, which was not significantly different from their value at 98 days (p = 0.48).

Supporting Information File 2.

A.

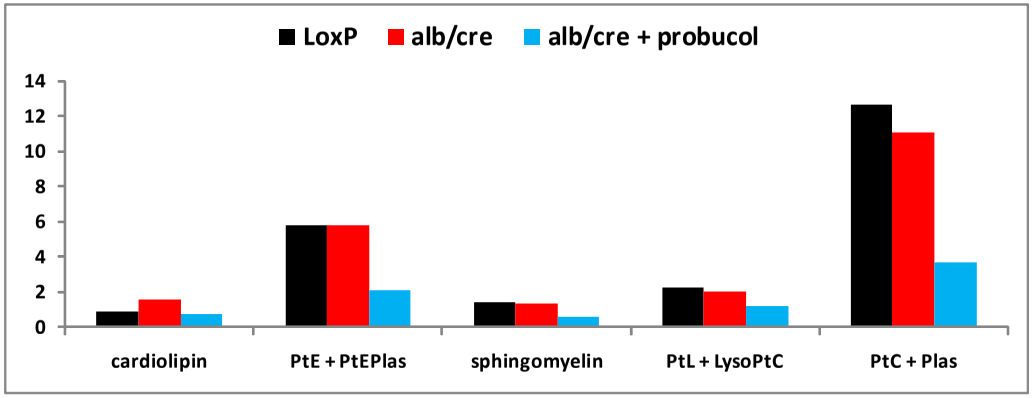

B.

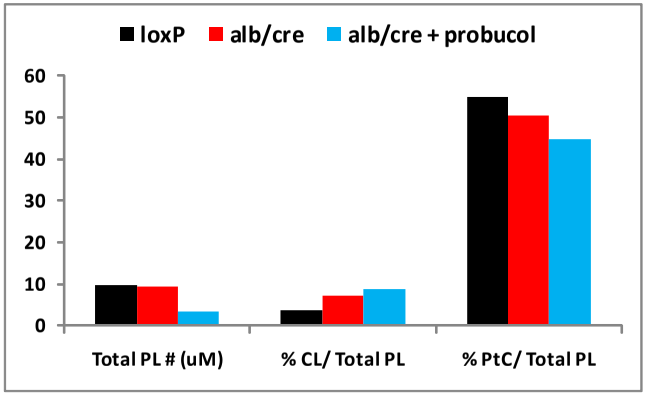

C.

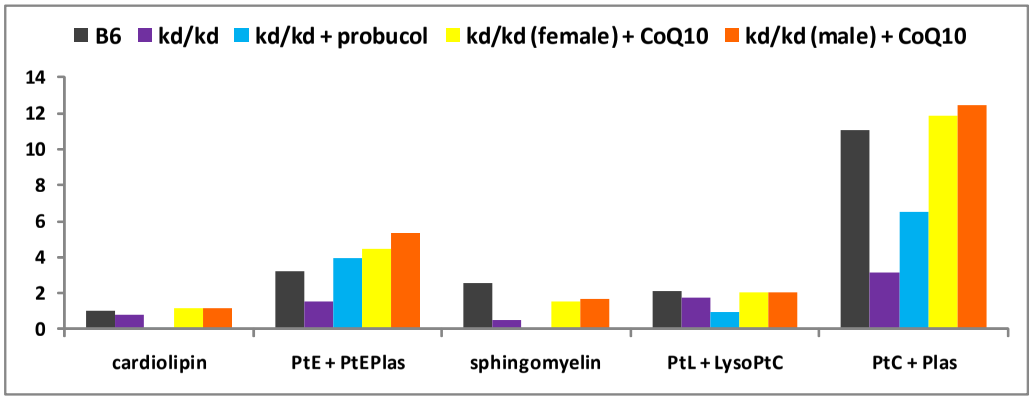

D.

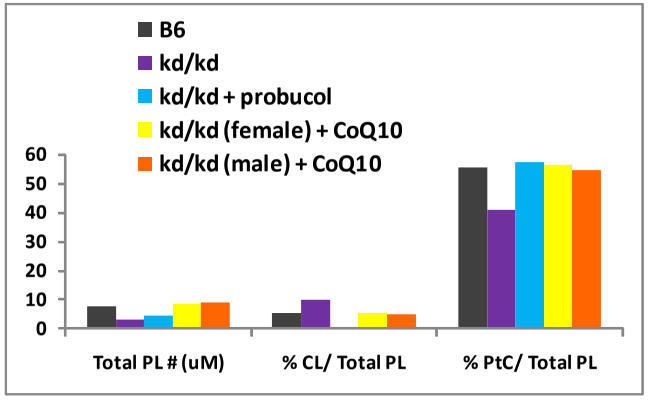

Supporting Information File 3.

A.

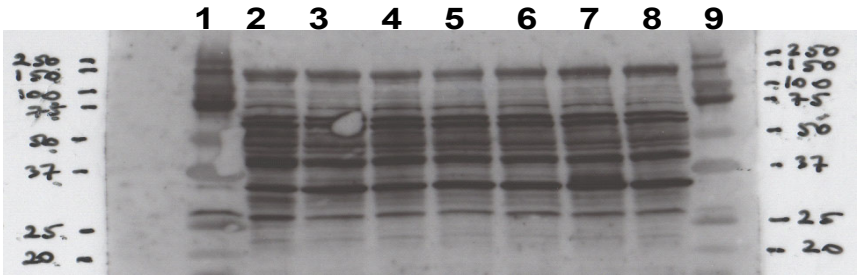

1: Prec Plus Kal.	Standard	20 ul
2: Wild-type (CD1)	235 days F	40 ug liver mito
3: B6 (1257)	184 days M	40 ug liver mito
4: kd/kd (37-2411)	154 days M	40 ug liver mito
5: B6 (1265)	165 days M	40 ug liver mito
6: kd/kd (37-2400)	148 days M	40 ug liver mito
7: B6 (1256)	188 days M	40 ug liver mito
8: kd/kd (37-2397)	150 days M	40 ug liver mito
9: Prec Plus Kal.	Standard	10 ul

B.

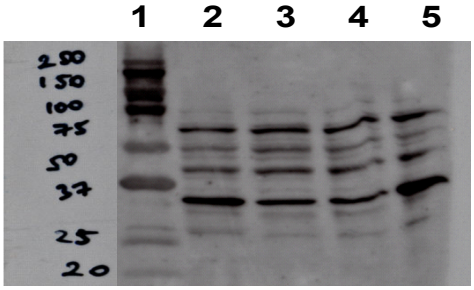

1: Prec Plus Kal.	Standard	10 ul
2: loxP (Lox-95)	140 days M	20 ug liver mito
3: alb/cre (Alb-67)	213 days M	20 ug liver mito
4: alb/cre (Alb-69)	178 days M	20 ug liver mito
5: kd/kd (37-2381)	124 days M	20 ug liver mito

C.

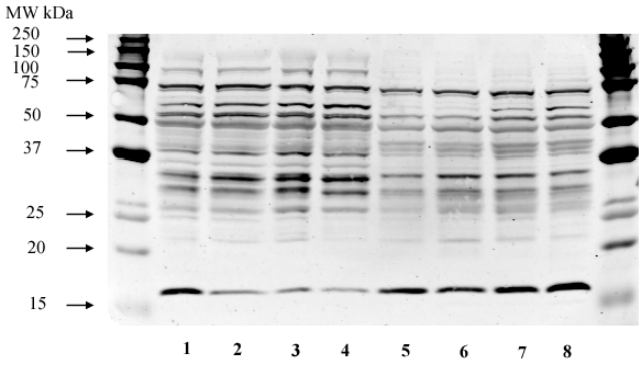

D.

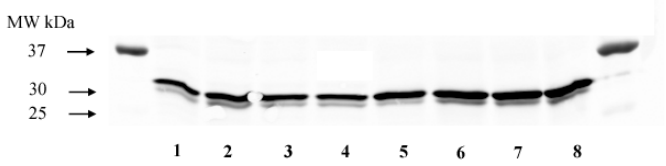

Supporting Information File 4.

Mouse Strain	N	Age (days)	Treatment	ALT (U/L)	Glucose (mM)	Urea (mM)	Ammonia (nM/ml)
LoxP	4	116 ± 5.5	control	14.4 ± 0.8	6.1 ± 1.0	5.7 ± 0.3	171 ± 41.8
LoxP	3	330 ± 0	control	19.9 ± 6.8	5.8 ± 0.6	4.6 ± 0.2	248 ± 36.0
LoxP	**[7**	**208 ± 115**	**control**	**16.7 ± 7.7**	**6.0 ± 1.9**	**5.2 ± 1.5**	**204 ± 101.9]**
alb/cre	**4**	**276 ± 36**	**control**	**14.7 ± 1.7**	**7.2 ± 0.9***	**4.9 ± 0.5**	**136 ± 22.0**
alb/cre	5	264 ± 0	probucol	16.0 ± 6.0	5.7 ± 1.3	5.3 ± 0.4	65 ± 16.0***,%
alb/cre	3	330 ± 52.0	probucol	15.2 ± 2.6	5.4 ± 0.7#	4.7 ± 0.7	139 ± 22.8
alb/cre	**[8**	**289 ± 44.0**	**probucol**	**15.9 ± 5.0**	**5.6 ± 1.0#**	**5.0 ± 0.6**	**92 ± 42.2***]**

Supporting Information File 6.

A.

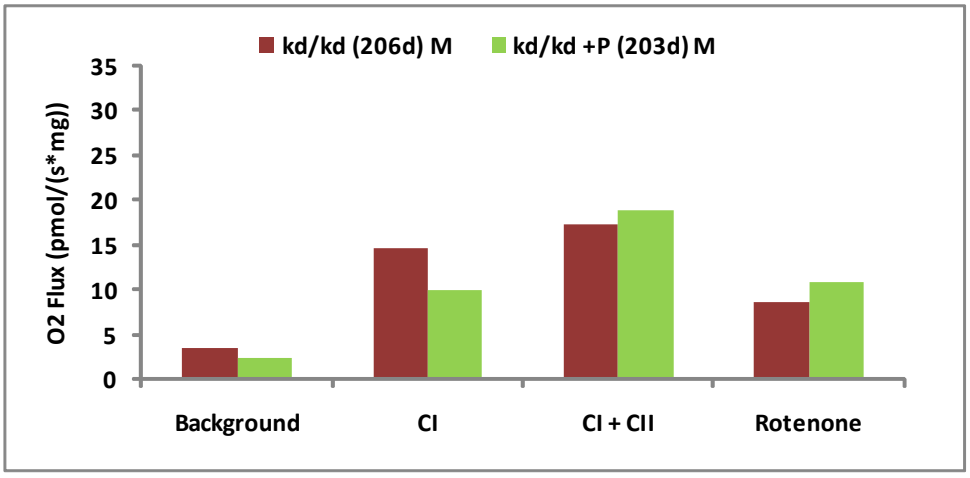

B.

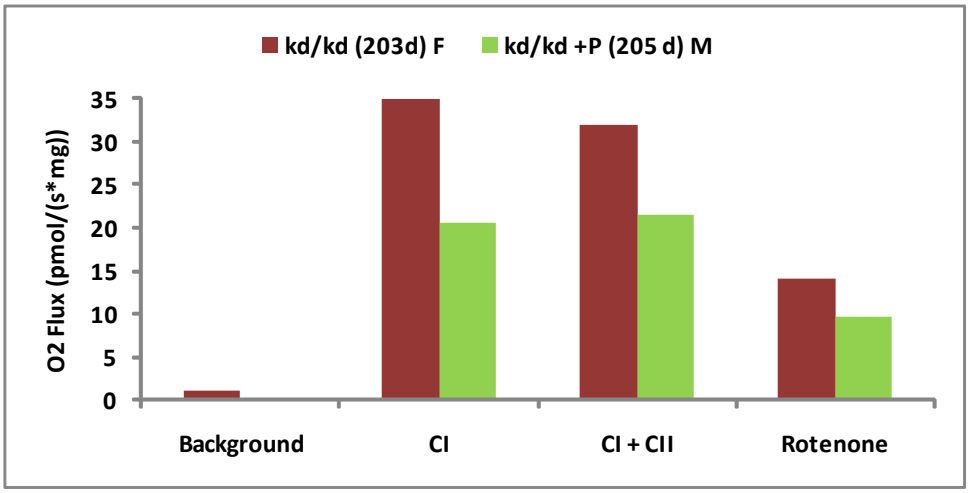

Supporting Information File 9.

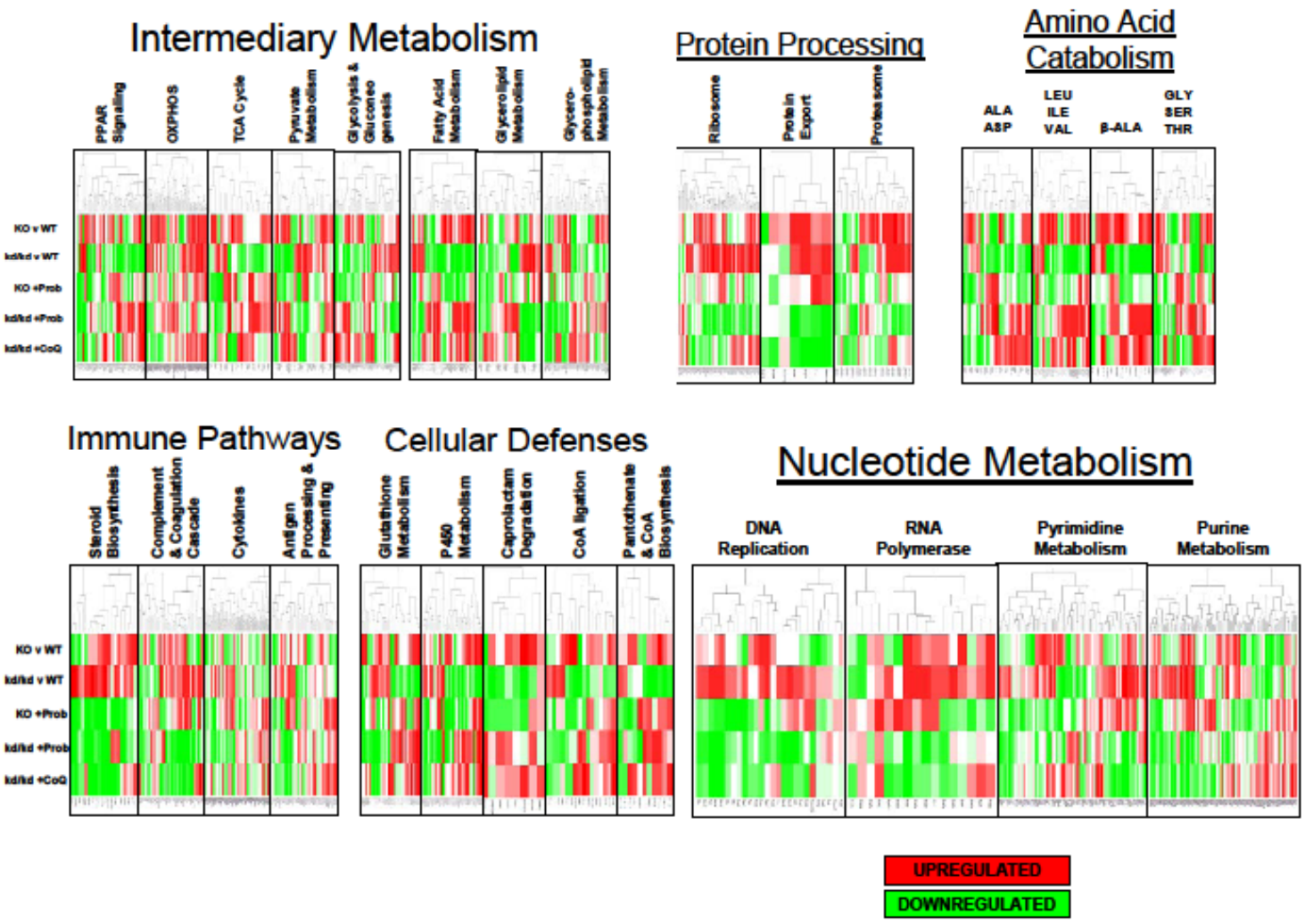

Supporting Information File 10.

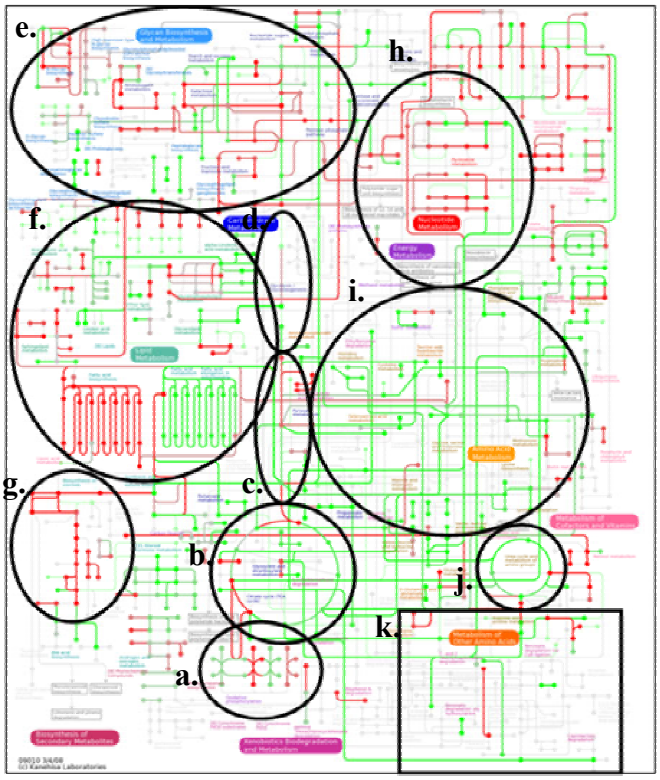

A. MISSENSE vs WT

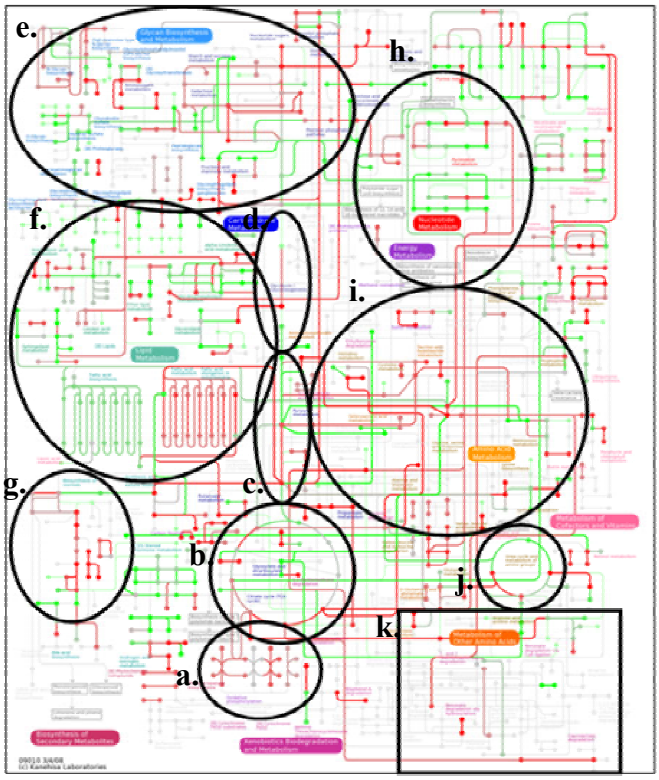

B. ALB/CRE KO vs WT

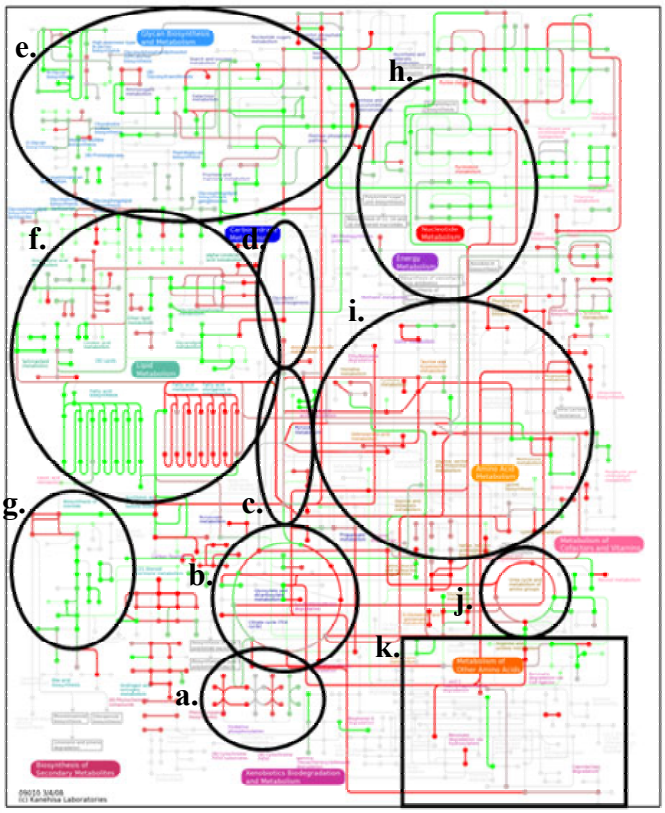

C. MISSENSE: Probucol vs Untreated

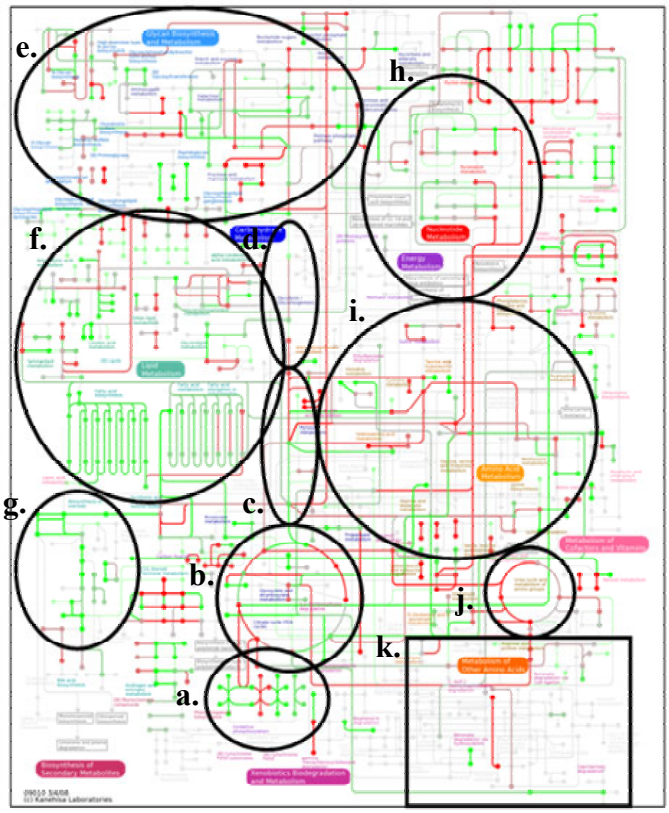

D. ALB/CRE KO: Probucol vs Untreated

Supporting Information File 11.

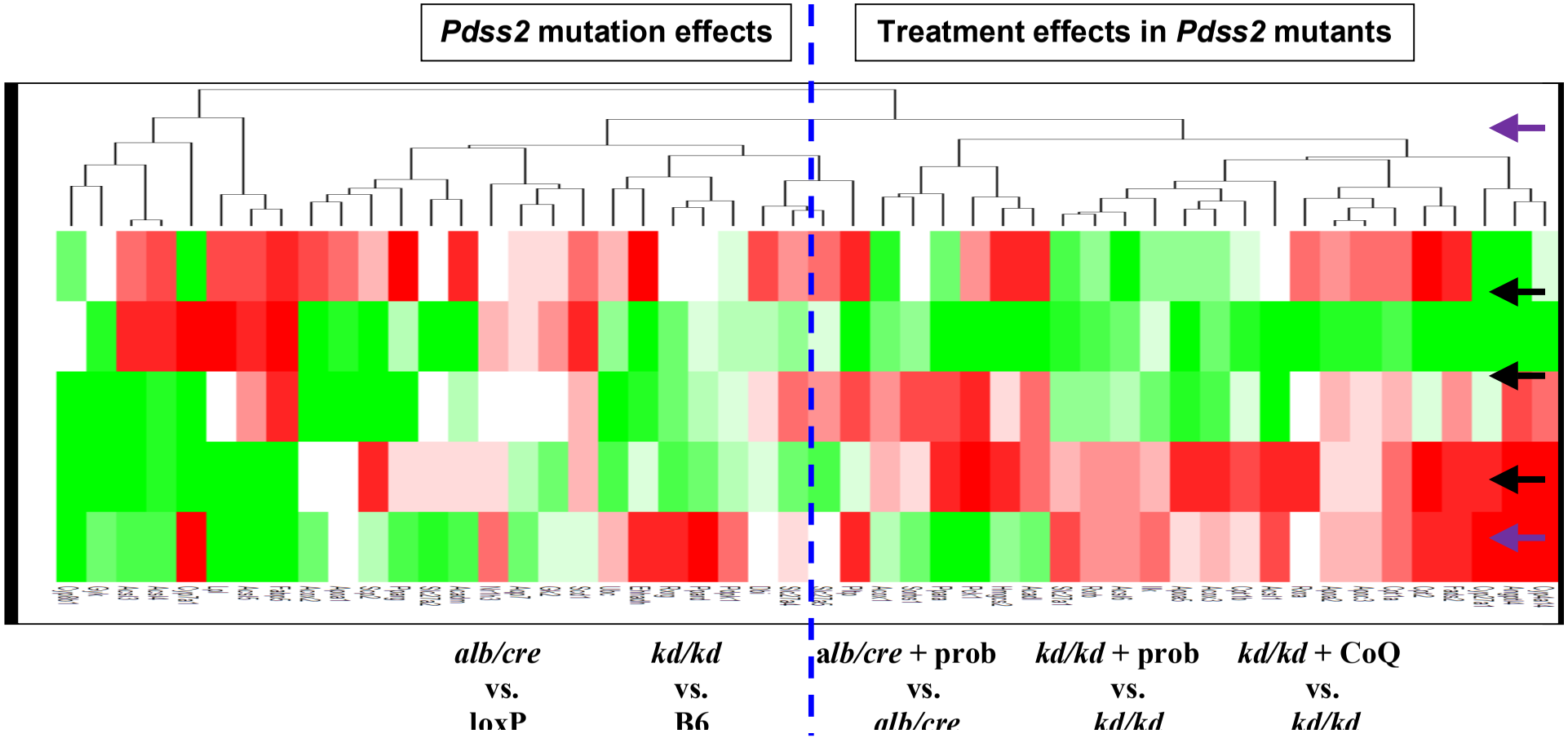

Supporting Information File 12.

	Probucol Treatment	Age (days)	Urine albumin	Nephritis score	Total Q Content (pmol/mg protein) Q9	Q10
FEMALE B6.*Pdss2*$^{kd/kd}$ MICE						
37-3234	No	215	40.96	4	83.21	1.9
37-3246	No	205	39.32	3	39.30	0.8
AVG +/- Std Dev					63.25 +/- 23.98	1.41 +/- 0.63
37-3212	Yes	207	22.12	2	71.28	2.41
37-3213	Yes	207	28.77	2	61.30	2.47
37-3214	Yes	207	6.14	1	94.67	3.8
AVG +/- Std Dev					76.60 +/- 19.24	2.95 +/- 0.80
*P value					0.1156	**0.0031**
MALE B6.*Pdss2*$^{kd/kd}$ MICE						
37-3244	No	205	81.92	3	39.15	0.59
37-3248	No	205	38.5	2	30.78	0.67
AVG +/- Std Dev					34.97 +/- 5.27	0.63 +/- 0.080
37-3215	Yes	205	0.69	1	66.97	2.96
37-3216	Yes	205	0.53	1	49.85	1.84
37-3217	Yes	205	0.81	1	46.03	1.55
37-3218	Yes	205	0.92	0	42.00	1.35
37-3219	Yes	205	0.85	0	49.68	2.23
AVG +/- Std Dev					54.68 +/- 17.81	2.02 +/- 0.80
*P value					**< 0.0001**	**<0.0001**

*compared to same sex untreated animals

Supporting Information File 13 – ADDITIONAL METHODS:

A. Measurement of CoQ content in kidney and liver. Kidney and liver homogenates were prepared as described previously (Saiki et al, 2008). Diethoxy-Q_{10} was synthesized as described previously (Edlund, 1988) and used as an internal standard. A known amount of diethoxy-Q_{10} was added to all samples and calibration curve standards before lipid extraction. The same amount of diethoxy-Q_{10} was also added to the CoQ_9 and CoQ_{10} standards prepared at different concentrations to generate an extracted standard curve. Lipid extractions were then performed on CoQ_9 and CoQ_{10} standards, and mouse tissue homogenates as described (Saiki et al, 2008). Dried lipids were suspended in ethanol and separated by reverse-phase HPLC with a Luna pentafluorophenyl (PFP2) column (Phenomenex; 5-µm, 50 × 3.0 mm). The mobile phase consisted of methanol/2-propanol (95/5) with 2.5 mM ammonium formate (solution A) and 2-propanol with 2.5 mM ammonium formate (solution B). At the time of injection, the mobile phase was 100% solution A (0.30 ml/min). After 2 minutes, solution B was increased linearly from 0 to 10% and the flow rate increased to 0.60 ml/min over a course of 3 minutes and returned to initial conditions at 5 minutes. CoQ_9, CoQ_9H_2, and CoQ_{10} and $CoQ_{10}H_2$ were quantified with an Applied Biosystems-MDS Sciex 4000 Q Trap (Hybrid triple-quad linear ion trap analyzer with autosampler, and a Turbo-V source equipped with ESI and APCI sources). The mass spectrometer was set to the positive ion mode with the parameters described previously (Marbois et al, 2010). The samples were analyzed in the multiple reaction monitoring (MRM) mode with the following transitions (*m/z*): 812.6/197 (ammonium adduct of Q_9); 814.6/197 (ammonium adduct of reduced Q_9H_2); 880.7/197 (ammonium adduct of Q_{10}); 882.7/197 (ammonium adduct of reduced $Q_{10}H_2$); 908.7/225 (ammonium adduct of diethoxy-Q_{10}); and 910.7/225 (ammonium adduct of diethoxy-$Q_{10}H_2$); however, the amount of diethoxy $Q_{10}H_2$ was negligible in these studies. Optimal settings for compound dependent parameters are in volts, and dwell in milliseconds: DP; declustering potential, EP; entrance potential, CE; collision energy, CXP; collision cell exit potential (DP;EP;CE;CXP;Dwell): Q_9 and Q_9H_2 (66;10;29;16;180); Q_{10}, and $Q_{10}H_2$ (86;10;35;10;180); diethoxy- Q_{10} and diethoxy-$Q_{10}H_2$, (76;10;29;12;180). Quantification of quinones utilized Analyst software version 1.4.2 (Applied Biosystems/MDS Sciex). Assays were performed by L.X.X., R.C.H., and B.M.

B. Blood analyte quantitation. Blood was obtained following a 4 hour fast by retro-orbital puncture, collected in heparinized tubes, and immediately centrifuged at top speed x 10 minutes at room temperature to obtain plasma. Plasma triglyceride and cholesterol levels were measured by use of the Stanbio kit (Boerne, Texas) in the Mouse Phenotyping, Physiology & Metabolism Core of the University of Pennsylvania. Plasma ALT concentration was also measured in the Mouse Phenotyping, Physiology, & Metabolism Core. Plasma glucose was quantified enzymatically using glucose oxidase (Bergmeyer et al, 1974). Ammonia and urea were assayed by standard methods (Geyer & Dabich, 1971; Nissim et al, 2005).

C. Liver lipid content analysis by NMR. Sample preparation and ^{31}P-NMR analysis were performed as previously described (Nissim & Weinberg, 1996). Briefly, mouse liver was immediately frozen upon dissection with liquid nitrogen cold clamps packed in foil and stored at -80°C. Frozen liver was then added to pre-weighed 15 ml tubes containing 10 ml of 2:1 by volume chloroform:methanol mixture per 0.5-1 gram of tissue and homogenized in a 15 ml Tenbroeck Tissue Grinder. Samples were placed overnight in a 37°C rotary shaker at 220 rpm in 15 ml tubes. Following centrifugation at 400 *g* for 20 minutes, supernatants were collected in pre-weighed 15 ml glass tubes and dried for 4 hours under nitrogen flow to protect from oxidation. Tubes were reweighed to calculate lipid mass. Lipid analysis was performed by NMR by Suzanne Wehrli, Ph.D., in the NMR core facility at The Children's Hospital of Philadelphia.

D. Liver total RNA isolation and expression microarray hybridization. Total RNA from each mouse liver was isolated by Trizol extraction (Invitrogen, CA), purified, and combined into a single aliquot from 100 mg flash-frozen liver specimens collected at the time of sacrifice, as previously described (Peng et al, 2008). Total RNA 260/280 and 260/230 > 1.8 was required for downstream analyses. For analysis of probucol and CoQ_{10} supplementation effects in B6.*Pdss2*$^{kd/kd}$ missense mutant mice, total RNA was individually hybridized to 20 total Illumina Mouse WG-6 v2.0 arrays, which included 5 biological replicates from each of 4 groupings: untreated B6.*Pdss2*$^{kd/kd}$ missense mutant mice, probucol-treated B6.*Pdss2*$^{kd/kd}$ mice, CoQ_{10}-treated B6.*Pdss2*$^{kd/kd}$ mice, and untreated B6 wild-type mice (GEO Accession No.: GSE27954). Probucol effects in

B6.*Alb/cre,Pdss2*$^{loxP/loxP}$ liver-conditional knockout mice (1 male and 1 female fed probucol-chow vs. 1 male and 1 female fed standard chow) was assessed by analysis of total RNA individually hybridized to Affymetrix 430 2.0 (3' biased) expression platform (GEO Accession No.: GSE18677) (Zhang et al, 2010). Results were compared to pathway expression alterations previously reported on the same platform for 3 B6.*Alb/cre,Pdss2*$^{loxP/loxP}$ liver-conditional knockout mice relative to 3 B6.*Pdss2*$^{loxP/loxP}$ wild-type controls (Peng et al, 2008) (GEO Accession No.: GSE10904). All RNA labeling and microarray hybridization was performed per manufacturer directions in the CHOP Nucleic Acid and Protein Core Facility.

E. Processing and bioinformatics analysis of microarray data. Data processing was mainly performed within the R statistical environment (www.r-project.org). Affymetrix data were processed by the RMA method (Irizarry et al, 2003) using a custom library file that re-mapped probes to the current version of Entrez gene (Dai et al, 2005). Illumina data output by BeadStudio software was processed by Loess normalization and averaged into 20,879 unique Entrez genes. All microarray data generated in this study is publicly available from the NCBI GEO database, as detailed above. The differential expression of genes was calculated as the log2 ratio of group means. Genes were ranked for each pair-wise comparison. Gene-to-pathway mapping information was downloaded from the Kyoto Encyclopeida of Genes and Genomes (KEGG) web site (www.genome.jp/kegg/). Two functional annotation tools, KEGG Atlas and GSEA, were applied to the ranked gene lists for pathway analysis. GSEA v2.0 (www.broad.mit.edu/gsea) was used to draw statistical conclusions about the modification of metabolic pathway by mutation or drug treatment. KEGG Atlas (www.genome.jp/kegg/atlas.html) was used to visualize differential gene expression on a well-organized map of intermediary metabolism.

F. PPARα and PPARγ relative expression analysis in mouse liver. The same mouse liver RNA samples used for microarray analyses were studied by relative quantitation of *PPARα* and *PPARγ* gene expression. 10 ug RNA was DNAse treated using TURBO DNA-free kit (#AM1907, Ambion Inc., Austin, TX). DNAse-treated total RNA was reverse transcribed in 20 ul reactions to generate cDNA using High Capacity cDNA Reverse Transcription Kit (#4368814, Applied Biosystems, Foster City, CA). 40 ng cDNA was used per

quantitative PCR reaction with Taqman Gene Expression Assays (Applied Biosystems) for the endogenous control (mouse β-actin Mm02619580_g1) and target genes *PPARα* (mouse Mm00627559_m1) and *PPARγ* (mouse Mm00440940_m1). Analyses were performed on an Applied Biosystems SDS-7500 Fast Sequence Detection System (SDS) qPCR machine. 7500/7500 Fast Sequence Detection Software version 2.0.1 was used for relative quantitation of gene expression. All analyses were performed by E.O. and E.P.

G. MnSOD relative expression analysis in mouse liver and kidney. Total RNA isolated from flash-frozen liver and kidney was prepared immediately following euthanasia by standard Trizol protocol (Invitrogen Corporation, Carlsbad, CA), as above. Total RNA analysis was performed as above with the exception that MnSOD was used as the target gene (mouse *SOD2* Mm00449726_m1 Applied Biosystems, Foster City, CA). Sequence Detection Software v.1.2.3 was used for relative quantitative analysis of gene expression. All analyses were performed by a single individual (E.P.).

H. MnSOD enzyme activity analysis in mouse liver and kidney isolated mitochondria. Mitochondria samples were isolated from mouse liver and kidney, as previously described (Peng et al, 2008). MnSOD activity assay was measured in frozen mitochondria as described by McCord and Fridovich (McCord & Fridovich, 1969), with slight modification (Dingley et al, 2009). All analyses were performed by a single individual (E.P.).

I. Immunoanalysis of 4-HNE protein adducts from liver and kidney isolated mitochondria. Intact liver mitochondria was isolated and immediately frozen in -80°C, as previously described (Peng et al, 2008). Frozen mitochondria were thawed on ice and subjected to Western blot analysis of 4-hydroxy-2-nonenal (4-HNE) protein adducts, as previously described (Catala, 2009; Dingley et al, 2009). Isolated mitochondria was diluted with Laemmli sample buffer containing β-mercaptoethanol, in 1:1 ratio and boiled at 98-100^{0}C for 4 minutes. Mitochondrial proteins were subjected to Western Blot analysis of lipid peroxidation as assessed by the level of 4-hydroxy-2-nonenal (4-HNE) protein binding. Equal amounts of mitochondrial protein (40 μg) were separated on 12% SDS-PAGE and transferred to nitrocellulose membranes. Resolved proteins were labeled with rabbit

anti-4-HNE (4-hydroxy-2-nonenal) antibody (Alpha Diagnostic International, San Antonio, TX) in 1:500 dilutions. Porin monoclonal antibody (VDAC1, voltage dependent anion channel) (MitoSciences, Eugene, OR) in 1ug/ml dilution was used as a loading control. Proteins were detected with Infrared IRDYE 680 conjugated goat anti-rabbit IgG for 4-HNE and IRDYE 800CW conjugated goat anti-mouse IgG in 1:10000 dilution and protein bands were visualized by scanning the membranes with Odyssey Infrared Imaging Systems (LI-COR Biosciences, Lincoln, NE). All analyses were performed by a single individual (E.P.).

J. Aconitase activity assay in isolated mitochondria. Intact liver mitochondria was isolated and immediately frozen in -80°C, as previously described (Peng et al, 2008). Freshly thawed mitochondrial aliquots were diluted to 10 mg/ml in 50 mM Tris-HCl pH 7.4 containing 2 mM sodium citrate and 0.6 mM $MnCl_2$, and then sonicated for 5 seconds. Then samples were further diluted to 2.5 mg/ml in the same buffer but containing 2.5 mM cysteine and 40 μM ferrous ammonium sulfate. Samples were then incubated for one hour on ice to activate aconitase in the sample prior to the assay. Aconitase activity was measured by monitoring absorbance at 340 nm in a freshly prepared reaction mixture containing 0.2 mM $NADP^+$, 5 mM sodium citrate, and a 1-unit/ ml concentration of pig heart isocitrate dehydrogenase in 50 mM Tris-HCl pH 7.4 plus 0.6 mM $MnCl_2$ (adapted from (Gardner, 2002; Rose & O'Connell, 1967)). To start the assay, 10 μl of a freshly activated aconitase sample (25 μg of protein) were added to the reaction mixture pre-equilibrated at 25°C. Measurements at 340 nm were monitored at intervals of 5 minutes for one hour, and aconitase activity was calculated from the linear increase after a lag in NADPH formation by using an extinction coefficient for NADPH of 6.22×10^3 M^{-1} cm^{-1}. All analyses were performed by a single individual (E.N.O.).

K. Respiratory capacity analysis in permeabilized skeletal muscle from *Pdss2* mutants treated long-term with probucol. Immediately following euthanasia, skeletal muscle was dissected from the proximal hind limbs of male B6.*Pdss2*$^{kd/kd}$ mice fed regular chow or long-term probucol supplementation since birth. Skeletal muscle was collected in ice cold relaxing and biopsy preservation solution, BIOPS, which contained 10 mM Ca-EGTA buffer, 0.1 uM free calcium, 20 mM imidazole, 20 mM taurine, 50mM K-MES, 0.5 mM DTT, 6.56 mM

MgCl, 5.77 mM ATP, 15 mM phosphocreatine, pH 7.1. Permeabilized muscle fibers were freshly prepared for respiratory capacity analysis by high resolution polarography using an Oxygraph-2K (Oroboros, Austria), as previously described (Lemieux & Gneiger, 2008). 2-3 mg permeabilized fresh muscle tissue isolated from untreated and probucol-treated B6.*Pdss2*$^{kd/kd}$ mice were simultaneously run in parallel chambers on two consecutive days. Experiments were performed as previously described (Lemieux et al, 2009). Substrates and inhibitors were added to the permeabilized muscle tissue in the following order: glutamate 20 mM, malate 10 mM, adenosine diphosphate (ADP) 0.2 mM, cytochrome C 10 uM, succinate 20 mM, carbonyl cyanide-p-trifluoromethoxyphenylhydrazone (FCCP) step-wise titration in 0.25 uM increments, rotenone 0.5 uM, and antimycin A 2.5 uM. Data was analyzed using DatLab4 (Oroboros, Austria).